The Role of Caretakers in Disease Dynamics

Charleston Noble · James P. Bagrow · Dirk Brockmann

Abstract One of the key challenges in modeling the dynamics of contagion phenomena is to understand how the structure of social interactions shapes the time course of a disease. Complex network theory has provided significant advances in this context. However, awareness of an epidemic in a population typically yields behavioral changes that correspond to changes in the network structure on which the disease evolves. This feedback mechanism has not been investigated in depth. For example, one would intuitively expect susceptible individuals to avoid other infecteds. However, doctors treating patients or parents tending sick children may also *increase* the amount of contact made with an infecteds, in an effort to speed up recovery but also exposing themselves to higher risks of infection. We study the role of these *caretaker* links in an adaptive network models where individuals react to a disease by increasing or decreasing the amount of contact they make with infected individuals.

We find that, for both homogeneous networks and networks possessing large topological variability, disease prevalence is decreased for low concentrations of caretakers whereas a high prevalence emerges if caretaker concentration passes a well defined critical value.

Keywords Complex networks · Adaptive networks · Social networks · Epidemics · Disease dynamics

1 Introduction

Physicists have taken numerous approaches to modeling infectious diseases, ranging from simple, deterministic compartmental models that qualitatively describe disease dynamics in single populations [4], to highly complex, stochastic metapopulation models that can account for the spread of emergent infectious diseases on a global scale [13, 14, 27]. Simple

C. Noble
Northwestern University, Evanston, IL 60208, USA

J.P. Bagrow · D. Brockmann (✉)
Engineering Sciences and Applied Mathematics, Northwestern Institute on Complex Systems,
Northwestern University, Evanston, IL 60208, USA
e-mail: brockmann@northwestern.edu

models, designed to investigate the basic mechanisms underlying disease dynamics, typically assume that a population is well-mixed, that interacting individuals are identical and that stochastic effects are negligible [3, 9]. On the other hand, complex computational models are manufactured to predict the time-course of actual emergent infectious diseases such as H1N1 in 2009 [5], SARS in 2003 [18] quantitatively. They typically take into account data on social variability, age structure, spatial heterogeneity, seasonal variation of disease dynamic parameters, multi-scale mobility networks, and account for stochastic effects. Both classes of models fulfill equally important, complementary, but almost mutually exclusive purposes.

Theoretical epidemiology experienced a major thrust with the advent of complex network theory and its introduction into the field [1, 23]. The study of network properties substantially advanced our understanding of disease dynamic phenomena on multiple levels [25]. On one hand, networks were used as a model for inter-individual relationships (social networks) [22]. On the other hand, the network approach was applied on a larger scale, modeling mobility and transport between populations [10, 18].

The use of network theoretical concepts allowed researchers to investigate how topological properties of underlying networks shape the contagion processes that evolve on them [7, 11, 19, 21, 28]. In the context of epidemiology, mapping structural features of networks to properties of the spread of the disease substantially increased the predictive power of models and our understanding of epidemic phenomena.

Although it is intuitive and plausible that network features determine the spread of a disease, it is equally plausible that an epidemic reshapes the structure of the underlying networks. For example, in response to information on an ongoing epidemic, people may change their behavior. They may decide to wear face masks, avoid contacts, and travel less. Surprisingly, this feedback mechanism has been neglected even in some of the most detailed and sophisticated modeling approaches [13, 14]. Topological properties of social networks affect disease dynamics, and the disease then feeds back to change the topology of the network. In order to understand the dynamics of contagion phenomena in a population, it is vital to understand the consequences of this feedback mechanism.

Networks that change their structure in response to their environment are called *adaptive* [8, 15, 17, 20]. In a recent study, Gross et al. proposed a simple adaptive network scheme, based on a *rewiring* rule, to understand how individuals' behavioral changes impact on the time course of an epidemic. In this model, susceptible individuals are allowed to protect themselves from infection by rewiring their existing links [16]. Specifically, with probability w a susceptible breaks the relationship with an infected person and forms a new link to another, randomly selected susceptible. Despite the simplicity of this approach, the mechanism can generate an abundance of interesting phenomena including hysteresis and multi-stability.

Although this mechanism is attractive, the response to an ongoing epidemic in a population has many facets. Not only do individuals avoid other infected individuals (negative response). In many scenarios, individuals increase their interaction with infected individuals (positive response), particularly in hospital scenarios, and families in which individuals adopt the role of a caretaker. Potentially, these positive responses can facilitate disease proliferation in a population and yield a higher disease prevalence. However, caretaker activity can have a positive effect on infected individuals, for example by increasing a person's recovery rate. A key question is how these effects interact and under what circumstances caretaker activity has a net positive or negative effect and how these effects play out in different network topologies.

Here we propose and investigate these questions using an adaptive network model. We consider two types of networks. First, the generic Erdös-Rényi (ER) random network with

binomial degree distribution, where each pair of nodes is linked with constant probability p_{ER} [12, 23]. We also consider Barabási-Albert scale-free (SF) networks with power law degree distributions [6], which more closely mimic the heterogeneity in social interactions. Dynamics on scale-free networks have a number of important properties. For instance, they lack epidemic thresholds and are immune to random immunization due to strong connectivity fluctuations [6, 23–26]. Thus diseases on scale-free networks are difficult to avoid, and once they take hold, they are difficult to eradicate. For both classes of networks we observe a critical caretaker proportion which minimizes disease severity and beyond which additional caretakers increase disease prevalence. However, the parameter regime for which the right amount of care-takers yields disease extinction is much smaller in Barabási-Albert networks. We use ER and SF networks with the same average degree.

2 Model description

We consider a network with a constant number of nodes N, representing individuals in a population. Each node is either susceptible (S) or infected (I). We denote the state variable of node i by $x_i = 0$ or $x_i = 1$, corresponding to states S or I, respectively. A pair (i, j) of nodes share a weighted symmetric link $w_{ij} \geq 0$ representing their contact rate. Note that in general these contact rates can have any real non-negative value, unlike network models that are based on binary interactions. Susceptible nodes can become infected, and infected nodes can then become susceptible again upon recovery. This is the well-studied SIS (susceptible-infected-susceptible) model [2]. We also consider the SIR (susceptible-infected-recovered) model where infected individuals become immune to the disease upon recovery. Each link is designated either caretaker (C) or regular (R), and the fraction of C links is denoted p_c. We denote this signature of a link by $\sigma_{ij} = 1$ if the link is a caretaker link and $\sigma_{ij} = -1$ if it is regular. These two classes represent different ways of responding to an epidemic. Caretaker relationships cause nodes to increase their contact frequency w_{ij} if an attached node is infected, while regular relationships cause nodes to avoid each other (decreasing contact rates) as illustrated in Fig. 1a. At each time step a susceptible i can become infected by one of its infected neighbors with a probability p_i that increases with link weight. We assume that:

$$p_i = 1 - \exp(-\alpha_i \tau) \tag{1}$$

where τ is the propensity of disease transmission following a contact, and $\alpha_i = \sum_j w_{ij} x_j$ is the susceptible's contact rate with infecteds.

An infected individual i recovers with propensity β_i which yields the probability of recovery

$$r_i = 1 - \exp(-\beta_i) \tag{2}$$

We consider two scenarios: (1) Infected nodes recover at a uniform rate $\beta_i = \beta$ or (2) with variable probability. In the latter case, caretaker relationships increase a node's recovery probability β_i according to

$$\beta_i = \beta_0 + (\beta_1 - \beta_0) \frac{\sigma_i^n}{\sigma_0^n + \sigma_i^n}$$

where β_0 is the base recovery rate, and β_1 the enhanced recovery rate induced by the action of caretakers (Fig. 1b). The quantity σ_i represents the total exposure of an infected to
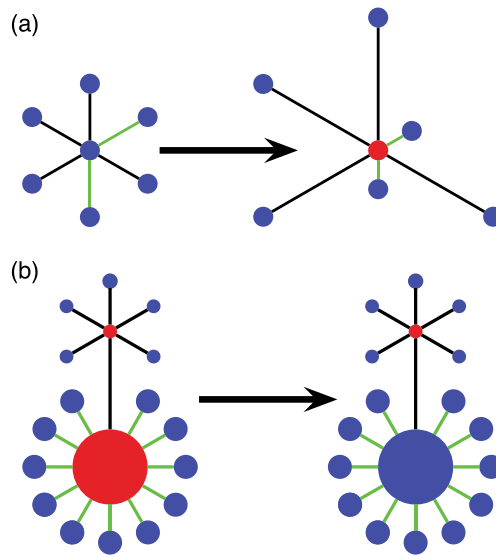
Fig. 1 (**a**) An initial network with all nodes susceptible (*left*) has two caretaker links (*green*) and three regular links (*black*). After the infection of the central node (shown by change to *red color*), regular-linked nodes react by "avoiding" the infected node (represented here by increasing distance). Caretaker-linked nodes, on the other hand, react by further increasing contact rates (represented here by decreasing distance). (**b**) Another network consists of two clusters around two central infected nodes (*red*). When considering the "caretaker effect", the more caretaker interactions (*green*) a node is exposed to, the greater its recovery rate (shown by node size; larger nodes have faster recovery rates). Thus after a time step, the lower infected node is more likely to recover, shown by its transition to susceptible status (*blue*) (Color figure online)

caretakers and is given by

$$\sigma_i = \frac{1}{2} \sum_j w_{ij}(1 + \sigma_{ij}),$$

thus σ_i is the total weight of caretaker interactions that node i experiences. The parameter σ_0 sets the scale for this exposure. The shape of the sigmoid curve can be controlled by the exponent n.

The infectious state of the system is defined by the states x_i of each node. We model the adaptive nature of the network weights w_{ij} according to

$$\delta_t w_{ij} = \mu \sigma_{ij}(x_i + x_j) - \gamma \left(w_{ij} - w_{ij}^0 \right). \tag{3}$$

Here the first term acts as the driving force of weight change, governed by the rate parameter μ. If a link is a caretaker link ($\sigma_{ij} = 1$), and one of the adjacent nodes is infected ($x_i = 1$ or $x_j = 1$), this term is positive and causes the weight to increase (if both nodes are infected the change is additive). Regular links ($\sigma_{ij} = -1$), on the other hand decrease in strength if one of the connected nodes is infected. The second term acts as a restorative force, governed by the rate parameter $\gamma \ll \mu$. Because we investigate a system in discrete time we use the following update rule for the weights:

$$w_{ij}(t+1) = w_{ij}(t) \exp\left[\mu \sigma_{ij}(x_i + x_j) \right.$$
$$\left. - \gamma \left(w_{ij}(t) - w_{ij}^0 \right) \right], \tag{4}$$

Fig. 2 Infected density ($I^* = I/N$) for SIS dynamics as a function of time for different caretaker proportions p_c, where caretakers do not improve recovery. Erdös-Rényi networks with adaptive rewiring were used (*solid lines*), as well as a similar static network (no rewiring, *dashed line*). Solid lines were obtained by averaging over 100 simulations, so a single-simulation plot is overlaid in each adaptive scenario for reference. The plot corresponds to $I_0 = 10^2$, $N = 10^3$, $p_{ER} = 0.008$, $\mu = 0.05$, $\gamma = 0.037$, $\beta = 0.15$, $\tau = 0.18$
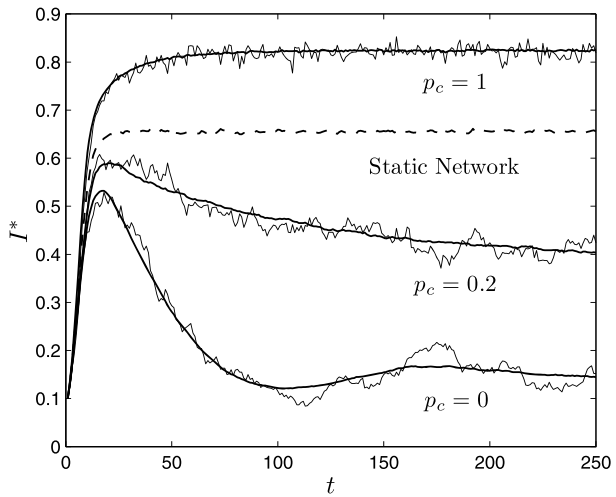
a discrete time reformulation of Eq. (3). These adaptive mechanisms are deterministic, while most existing models consider stochastic adaptation, and allows for efficient simulation compared with typical stochastic mechanisms. Likewise this model incorporates weighted links while previous models focus mainly on unweighted networks.

3 Results

We first consider SIS dynamics. At each time step, a randomly chosen node i can transition from S to I with probability p_i, or from I to S with probability r_i as given above. To study the effect of adaptive rewiring, we first consider a system without the caretaker effect on the recovery rate, i.e. $\beta_1 = \beta_0$. Caretakers only increase their interaction with infected individuals. We consider a network with weights initially distributed uniformly between 0 and 1. Results are shown in Fig. 2. In the absence of caretaker links ($p_c = 0$), the equilibrium endemic state $I^* = I_t/N$ is much lower than compared to the static network (without rewiring). This is expected, as only regular (negative) interactions exist that decrease in response to the epidemic. The total network weight adapts to a smaller value, decreasing the endemic state. The dynamics of the disease and adaptation of the network is visible in the damped oscillation of the fraction of infecteds. This is unusual as SIS models do not typically oscillate.

However, as the fraction of caretakers is increased, diseases can attain higher endemic states than their static network counterparts. The caretaker dynamics increases the interaction rate with infecteds, effectively yielding a higher disease prevalence, which is expected.

The system that lacks a positive caretaker effect represents a somewhat artificial limiting case. We therefore consider a positive *caretaker effect*: caretaker relationships lend higher recovery rates $\beta_1 > \beta_0$ to infected individuals, see Eq. (2). In particular, we consider the effect of varying the maximum recovery rate β_1 and the fraction of caretaker links p_c on the extinction probability p_{ext} of the disease. (We measure p_{ext} as the fraction of Monte Carlo realizations that finish with an empty infecteds compartment.) The results are depicted in Figs. 3 and 4. In general, increasing β_1 yields higher extinction, since caretaker links are more effective at raising recovery rates. One would then expect that increasing the caretaker proportion p_c would also yield higher extinction, as more relationships would cause

Fig. 3 Extinction probability p_{ext} for SIS dynamics as a function of caretaker proportion p_c for various values of β_1 in an Erdös-Rényi network. Note that extinction is maximized at $p_c \approx 0.1$ with a weak dependence on β_1. Approaching this value from the left yields a gradual increase in extinction, while increasing p_c past this critical value causes a rapid decrease in p_{ext}. The plot corresponds to $I_0 = 10^2$, $N = 10^3$, $\mu = 0.05$, $\gamma = 0.037$, $\tau = 0.18$, $\beta_0 = 0.35$, $\sigma_0 = \langle \sigma_i \rangle|_{t=0}$, $p_{ER} = 0.008$
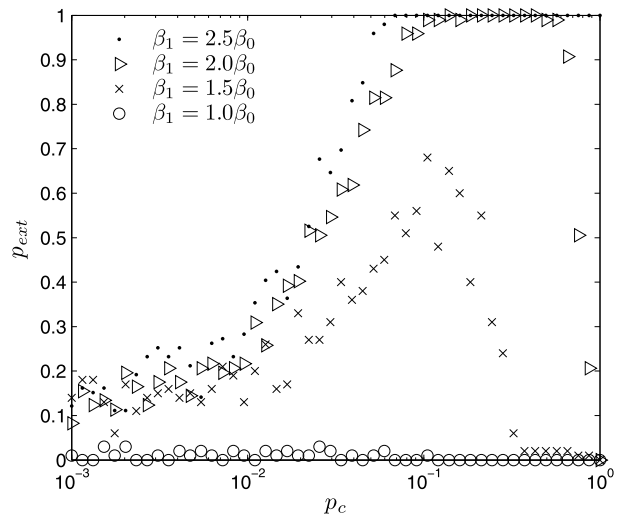
increasing recovery rates. However, this is not necessarily the case. Raising the caretaker proportion past some β_1-dependent critical value allows diseases to persist. This critical value also serves as a threshold, as increasing p_c above this value rapidly decreases the extinction probability to 0. This is illustrated in Fig. 3. Increasing p_c at first yields an increased p_{ext} until a maximum is reached. A further increase leads to a rapid decrease in extinction probability. For the Erdös-Rényi network, the critical fraction of caretakers is approximately $p_c \approx 10\,\%$. For p_c values above or below this, high extinction probability is seen only for very high values of β_1. Note however, that even for very small fractions of caretakers, a substantial increase in extinction probability is observed. This suggests that, if the caretaker-effect is taken into account, the best strategy to extinguish a disease is the existence of a few effective caretaker relationships, that safely avoids the negative effects that emerge beyond the critical concentration. Note also that for non-vanishing p_c, guaranteed extinction ($p_{ext} = 1$) is observed only for very high values of β_1.

Note that these results were obtained for an Erdös-Rényi network. In order to investigate the interaction of network adaptation in combination with strong network heterogeneity, we investigated the dynamics in a scale free (SF) topology. The results are also depicted in Fig. 4.

On these SF networks, we observe results quite similar to the ER system (also shown in Fig. 4). However, for a given β_1 in the SF system, the range of caretaker concentrations that yield extinction is much smaller than that observed for the ER system. In addition, for a given caretaker concentration, much higher values of β_1 are needed to yield extinction. Thus in SF systems, caretakers are largely ineffective except in finely-tuned concentrations with very high values of β_1. This contrasts with caretakers in ER systems which show positive effects for a large range of concentrations and β_1 values.

To explain these results, consider a susceptible node i and its total rate of interaction with infected neighbors:
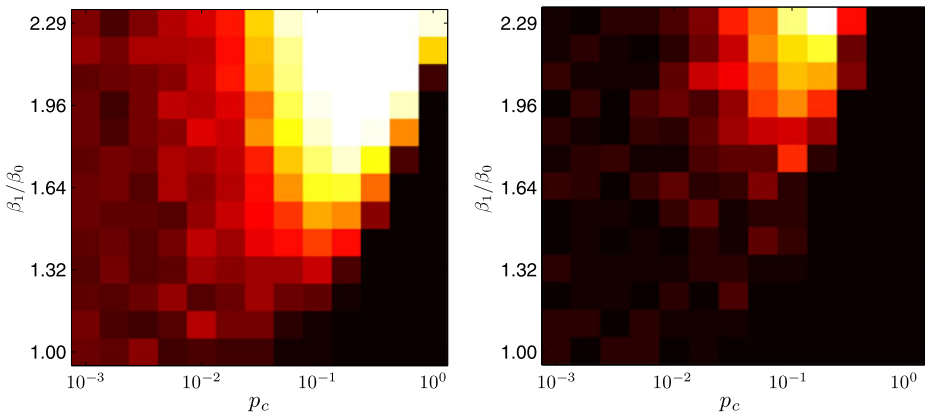
$$\Phi_{SI}(i) = \sum_j w_{ij} x_j.$$

Fig. 4 Two-parameter phase diagrams showing extinction probability for SIS dynamics as a function of maximum caretaker effectiveness β_1 and caretaker proportion p_c. Erdös-Rényi (*left*) and Barabási-Albert Scale-Free networks (*right*) were considered. In the black regions, extinction probability is 0 while extinction probability is 1 in the white regions. The plots suggest that increasing the caretaker proportion past a critical value yields a decreased extinction probability in both networks. We also see that $p_c \approx 10^{-1}$ yields maximum disease extinction probability. The plots correspond to $I_0 = 10^2$, $N = 10^3$, $\mu = 0.05$, $\gamma = 0.037$, $\tau = 0.18$, $\beta_0 = 0.35$, $\sigma_0 = \langle \sigma_i \rangle|_{t=0}$ if $\langle \sigma_i \rangle|_{t=0} > 0$ otherwise $\beta_i = \beta_0$, and a mean degree $k_0 = 4$ for both Erdös-Rényi and Scale-Free networks

The ratio of *SI* interaction rates and total equilibrium interaction rate $\alpha_0 = \langle \sum_{i<j} w_{ij} \rangle$ is given by

$$\alpha_{SI} = \frac{1}{\alpha_0} \sum_i \Phi_{SI}(i)(1 - x_i).$$

Averaging this measure over the time-course of a disease gives us a measure of the typical fraction of contacts due to SI interaction:

$$\langle \alpha_{SI} \rangle = \frac{1}{T\alpha_0} \int_0^T dt \left[\sum_{i,j} (1 - x_i) w_{ij} x_j \right].$$

Now consider this time averaged $\langle \alpha_{SI} \rangle$ as a function of p_c for various values of β_1, see Fig. 5. For $\beta_1 = \beta_0$ (i.e. no caretaker effect on recovery rates), the rate of *SI* interactions increase steadily as p_c is increased, yielding a more stable endemic state and high prevalence. When the caretaker effect is taken into account, we observe an initial decrease of *SI* interactions. Increasing p_c further can result in increasing *SI* interactions, entering a regime in which a large fraction of caretaker links results in a negative effect.

Note that, for all scenarios pictured in Fig. 5, the SI contact fraction is higher in the SF system than its ER counterpart. Perhaps there exists some SI contact threshold above which diseases are able to persist. Then we see in Fig. 5 that simply more scenarios surpass this threshold in the SF system than the ER system, certainly consistent with and possibly explaining our results in Fig. 4.

Next we turn our attention to the effect of caretaker adaptive networks on systems that are better described by SIR dynamics. Here individuals (nodes) exist in one of three states, susceptible (*S*), infected (*I*) or recovered (*R*). Individuals can transition from *S* to *I* with probability p_i and from *I* to *R* with probability r_i, as given above in Eqs. (1) and (2). The state *R* is absorbing, so once all infected nodes in a population recover, the disease dies out
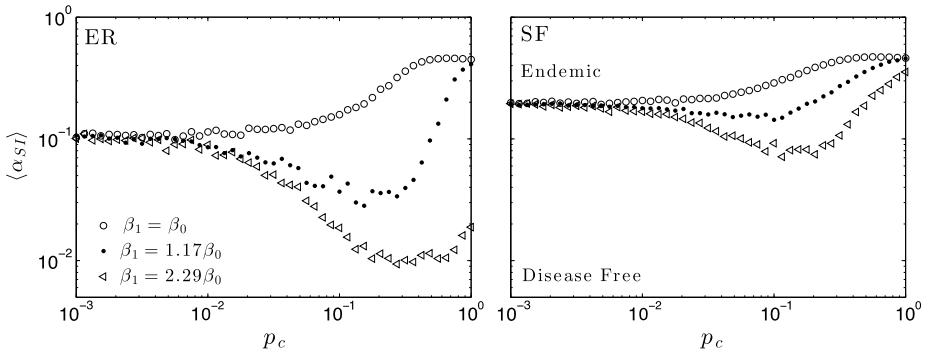
Fig. 5 Time-averaged SI contact fraction $\langle \alpha_{SI} \rangle$ for SIS dynamics with different values of the caretaker proportion p_c. Three β_1/β_0 values were chosen to correspond with low, intermediate, and high traces in the phase diagram of Fig. 4. An Erdös-Rényi network was used (*left*), as well as a Scale-Free network (*right*). The plots correspond to $I_0 = 10^2$, $N = 10^3$, $\mu = 0.05$, $\gamma = 0.037$, $\tau = 0.18$, $\beta_0 = 0.35$, $\sigma_0 = \langle \sigma_i \rangle |_{t=0}$ if $\langle \sigma_i \rangle |_{t=0} > 0$ otherwise $\beta_i = \beta_0$, and a mean degree $k_0 = 4$ for both Erdös-Rényi and Scale-Free networks

(see Fig. 6). In order to investigate the impact of caretaker dynamics and an SIR scenario, we focus on the *attack rate (ratio)* and the *epidemic peak*. The attack rate (AR) is simply the fraction of the population which contracts the infection at some point during the epidemic. Since every infected node eventually enters the recovered class, this is equivalent to the fraction of recovered nodes at the end of the epidemic:

$$AR = \frac{R_\infty}{N}$$

The epidemic peak (EP) is the maximum infected fraction attained in the population over the course of the epidemic. Figure 7 depicts the attack rate as a function of p_c for various values of the recovery rate parameter β_1. Interestingly, without a caretaker effect ($\beta_1 = \beta_0$) the increase in attack rate is not substantial as p_c is increased, implying that adaptation alone plays a minor role in SIR dynamics on ER networks. For $\beta_1 > \beta_0$, we observe a decrease in attack rate even for small fractions of caretaker links. The minimum attack rate is attained only in a regime where most links are caretaker links.

Figure 8 depicts the attack rate as a function of both system parameters β_1 and p_c and compares the behavior in both network architectures, Erdös-Rényi and Barabási-Albert. In contrast with the SIS system, network topology does not substantially change the dynamics, both networks exhibit a similar attack rate as a function of β_1 and p_c. For fixed β_1 increasing p_c first decreases the attack rate until a minimum is attained. Increasing p_c further increases the attack rate again.

The dynamics seen for the attack rate are mirrored in the epidemic peak *EP* as well (Fig. 9), which decreases as caretaker effectiveness (represented by β_1) increases. There is again a critical relationship with p_c, as values of $p_c \approx 0.2$ tend to minimize the epidemic peak for $\beta_1 > \beta_0$. Again though, for $\beta_1 = \beta_0$, increasing p_c yields a monotonic increase in *EP*.

4 Conclusions

Individual response can have a great impact on the dynamics of spreading diseases on complex networks. In particular, allowing individuals (caretakers) to become closer to infecteds
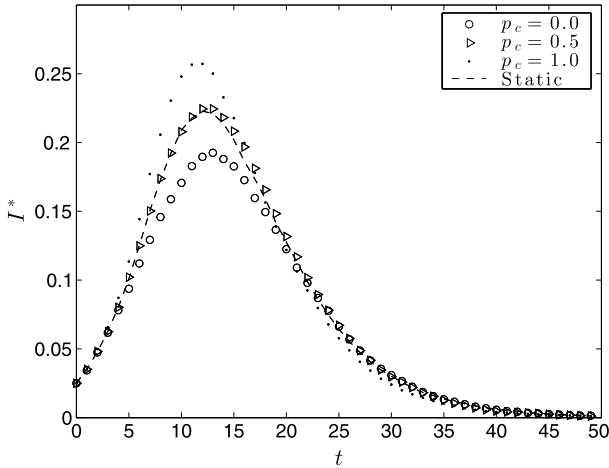
Fig. 6 Infected density ($I^* = I/N$) for SIR dynamics as a function of time for different caretaker proportions p_c. Erdös-Rényi networks with adaptive rewiring were used, as well as a similar static network (no rewiring, dashed line). Note that increasing p_c increases disease severity, in particular increasing both the epidemic peak and attack rate. This is as expected because caretakers have no positive effect. Note also that the static network corresponds roughly to the half caretaker/half regular scenario. In this scenario the harm caused by caretakers approaching infecteds is roughly offset by regulars avoiding infecteds, rendering the system similar to the static network. The plots correspond to $I_0 = 25$, $N = 10^3$, $\mu = 0.05$, $\gamma = 0.037$, $\tau = 0.45$, $\beta_0 = 0.20$, $\sigma_0 = \langle \sigma_i \rangle |_{t=0}$ if $\langle \sigma_i \rangle |_{t=0} > 0$ otherwise $\beta_i = \beta_0$, $n = 2$, $p_{ER} = 0.008$ (Erdös-Rényi). Scale-Free network results were similar

Fig. 7 Attack rate AR as a function of p_c for SIR dynamics with various values of β_1 in an Erdös-Rényi network. For each $\beta_1 > \beta_0$, the attack rate is minimized for some value of p_c between 10^{-1} and 10^0. As β_1 increases, this minimum point shifts subtly to the right. This shows that the more effective caretakers are at healing, the more caretaker relationships the system can permit before they have a negative impact on the attack rate. The plots correspond to $I_0 = 25$, $N = 10^3$, $\mu = 0.05$, $\gamma = 0.037$, $\tau = 0.25$, $\beta_0 = 0.20$, $\sigma_0 = \langle \sigma_i \rangle |_{t=0}$ if $\langle \sigma_i \rangle |_{t=0} > 0$ otherwise $\beta_i = \beta_0$, $n = 2$, $p_{ER} = 0.008$
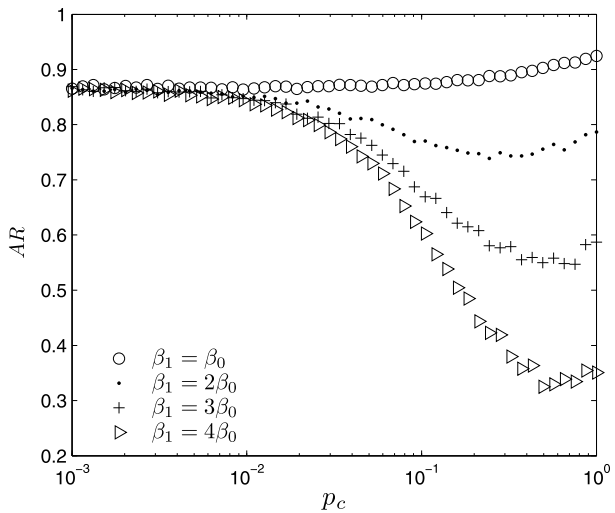
is a calculated risk. If the caretakers are not effective healers (such as non-physician parents and children), then the severity of the disease generally increases. But if the caretakers are effective healers (consider doctor/patient relationships, for example), then the outcome of the disease can be improved even by a small number of them. If too many caretakers are introduced, though, their healing benefit is overridden by their increased exposure, yielding a worse outcome than if the population had simply not reacted.
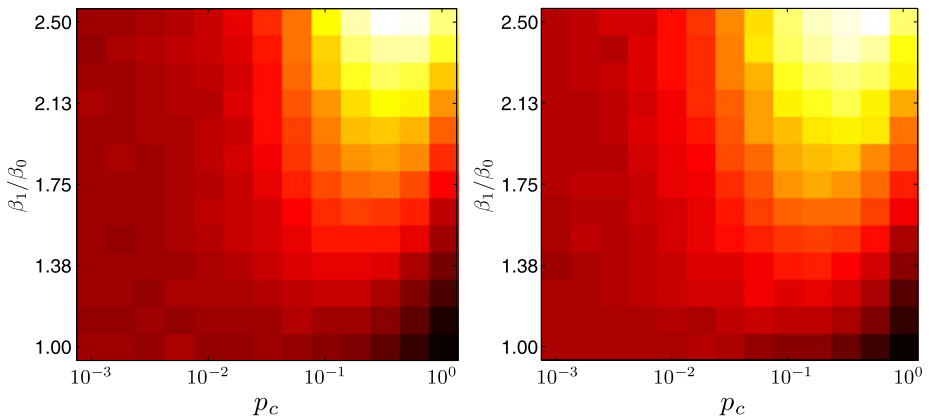
Fig. 8 Two-parameter phase diagrams showing the dependence of attack rate in SIR dynamics on maximum caretaker effectiveness β_1 (normalized by the baseline-recovery probability β_0) and caretaker proportion p_c. Erdös-Rényi (*left*) and Scale-Free (*right*) networks were considered. Attack rate approaches zero in the white regions, while it approaches 1 in the black regions. Note that increasing p_c yields lower attack rates for $p_c < 0.2$, but increasing past this critical value yields increasing attack rates. There is a critical value $p_c \approx 0.2$ at which attack rate is minimized for most values of β_1. Furthermore, this effect is seen in both ER and SF networks, though attack rates are lower overall on the SF network. The plots correspond to $I_0 = 25$, $N = 10^3$, $\mu = 0.05$, $\gamma = 0.037$, $\tau = 0.25$, $\beta_0 = 0.20$, $\sigma_0 = \langle \sigma_i \rangle|_{t=0}$ if $\langle \sigma_i \rangle|_{t=0} > 0$ otherwise $\beta_i = \beta_0$, $n = 2$, and a mean degree $k_0 = 4$ for both Erdös-Rényi and Scale-Free networks
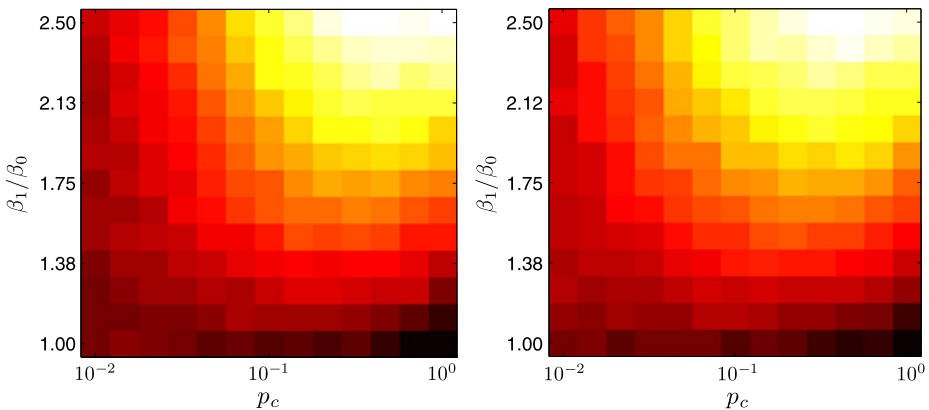

Fig. 9 Two-parameter phase diagrams showing the dependence of the epidemic peak (*EP*) in SIR dynamics on the maximum caretaker effectiveness β_1 (normalized by the baseline-recovery probability β_0) and caretaker proportion p_c. Erdös-Rényi (*left*) and Scale-Free (*right*) networks were considered. The epidemic peak approaches zero in the white regions, while it approaches 1 in the black regions. Note the similarities to the attack rate diagram in Fig. 8. The epidemic peak is minimized for $p_c \approx 0.2$ for most values of β_1, but for $p_c < 0.2$ or $p_c > 0.2$, the attack rate is greater for a given value of β_1. The plots correspond to $I_0 = 25$, $N = 10^3$, $\mu = 0.05$, $\gamma = 0.037$, $\tau = 0.40$, $\beta_0 = 0.20$, $\sigma_0 = \langle \sigma_i \rangle|_{t=0}$ if $\langle \sigma_i \rangle|_{t=0} > 0$ otherwise $\beta_i = \beta_0$, $n = 2$, and a mean degree $k_0 = 4$ for both Erdös-Rényi and Scale-Free networks

These findings have a number of implications in public health. For one, in a large-scale epidemic there certainly exists a critical fraction of doctors and aid workers in the population. If there are too few or too many, they can actually *increase* the total number of individuals infected over the course of the disease. Furthermore, diseases become more sensitive

to this critical fraction as interaction variability increases among the underlying population. And since social networks tend to display high interaction variability, real-world diseases should be particularly sensitive to this critical fraction. Thus in the face of an epidemic, fighting infection with caretakers likely will not be more effective than employing a natural avoidance strategy unless public health officials can precisely determine the optimal fraction of doctors and aid workers for their population.

References

1. Albert, R., Barabási, A.L.: Statistical mechanics of complex networks. Rev. Mod. Phys. **74**, 47–97 (2002)
2. Allen, L.J., Burgin, A.M.: Comparison of deterministic and stochastic sis and sir models in discrete time. Math. Biosci. **163**(1), 1–33 (2000)
3. Anderson, R.M., May, R.M.: Population biology of infectious-diseases 1. Nature **280**(5721), 361–367 (1979)
4. Anderson, R.M., May, R.M., Anderson, B.: Infectious Diseases of Humans: Dynamics and Control. Oxford Univ. Press, New York (1992)
5. Bajardi, P., Poletto, C., Ramasco, J.J., Tizzoni, M., Colizza, V., Vespignani, A.: Human mobility networks, travel restrictions, and the global spread of 2009 H1N1 pandemic. PLOS One **6**(1) (2011)
6. Barabási, A.L., Albert, R.: Emergence of scaling in random networks. Science **286**(5439), 509–512 (1999)
7. Barahona, M., Pecora, L.M.: Synchronization in small-world systems. Phys. Rev. Lett. **89**, 054,101 (2002)
8. Bornholdt, S., Rohlf, T.: Topological evolution of dynamical networks: global criticality from local dynamics. Phys. Rev. Lett. **84**, 6114–6117 (2000)
9. Brockmann, D.: Reviews of Nonlinear Dynamics and Complexity. Wiley-VCH, Weinheim (2010). SCHUSTER:REVIEWS 2 O-BK
10. Colizza, V., Pastor-Satorras, R., Vespignani, A.: Reaction-diffusion processes and metapopulation models in heterogeneous networks. Nat. Phys. **3**(4), 276–282 (2007)
11. Eguíluz, V.M., Klemm, K.: Epidemic threshold in structured scale-free networks. Phys. Rev. Lett. **89**, 108,701 (2002)
12. Erdos, P., Renyi, A.: On the evolution of random graphs. Magy. Tud. Akad. Mat. Kut. Intéz. Közl. **5**, 17–61 (1960)
13. Ferguson, N., Cummings, D., Cauchemez, S., Fraser, C., Riley, S., Meeyai, A., Iamsirithaworn, S., Burke, D.: Strategies for containing an emerging influenza pandemic in Southeast Asia. Nature **437**(7056), 209–214 (2005)
14. Ferguson, N.M., Cummings, D.A.T., Fraser, C., Cajka, J.C., Cooley, P.C., Burke, D.S.: Strategies for mitigating an influenza pandemic. Nature **442**(7101), 448–452 (2006)
15. Gross, T., Blasius, B.: Adaptive coevolutionary networks: a review. J. R. Soc. Interface **5**(20), 259–271 (2008)
16. Gross, T., D'Lima, C.J.D., Blasius, B.: Epidemic dynamics on an adaptive network. Phys. Rev. Lett. **96**, 208701 (2006)
17. Holme, P., Ghoshal, G.: Dynamics of networking agents competing for high centrality and low degree. Phys. Rev. Lett. **96**, 098701 (2006)
18. Hufnagel, L., Brockmann, D., Geisel, T.: Forecast and control of epidemics in a globalized world. Proc. Natl. Acad. Sci. USA **101**(42), 15124–15129 (2004)
19. Kuperman, M., Abramson, G.: Small world effect in an epidemiological model. Phys. Rev. Lett. **86**, 2909–2912 (2001)
20. Li, K., Fu, X., Small, M., Ma, Z.: Adaptive mechanism between dynamical synchronization and epidemic behavior on complex networks. Chaos **21**, 03311 (2011)
21. Lloyd, A.L., May, R.M.: How viruses spread among computers and people. Science **292**(5520), 1316–1317 (2001)
22. Newman, M.: Spread of epidemic disease on networks. Phys. Rev. E **66**(1), 016,128 (2002)
23. Newman, M.E.J.: The structure and function of complex networks. SIAM Rev. **45**(2), 167–256 (2003)
24. Pastor-Satorras, R., Vespignani, A.: Epidemic dynamics and endemic states in complex networks. Phys. Rev. E **63**, 066117 (2001)
25. Pastor-Satorras, R., Vespignani, A.: Epidemic spreading in scale-free networks. Phys. Rev. Lett. **86**, 3200–3203 (2001)

26. Pastor-Satorras, R., Vespignani, A.: Immunization of complex networks. Phys. Rev. E **65**, 036104 (2002)
27. Van den Broeck, W., Gioannini, C., Goncalves, B., Quaggiotto, M., Colizza, V., Vespignani, A.: The GLEaMviz computational tool, a publicly available software to explore realistic epidemic spreading scenarios at the global scale. BMC Infect. Dis. **11**, 37 (2011)
28. Xulvi-Brunet, R., Sokolov, I.M.: Reshuffling scale-free networks: from random to assortative. Phys. Rev. E **70**, 066102 (2004)